ELSEVIER

Brain Research Protocols 8 (2001) 16–24

BRAIN RESEARCH PROTOCOLS

www.elsevier.com/locate/bres

Protocol

Wavelet Transform in the analysis of the frequency composition of evoked potentials

R. Quian Quiroga[a,*], O.W. Sakowitz[b], E. Basar[c,e], M. Schürmann[d]

[a] *John von Neumann Institute for Computing, Forschungszentrum Jülich, D-52425 Jülich, Germany*
[b] *Department of Neurosurgery, Charité, Humboldt University Berlin, D-13353 Berlin, Germany*
[c] *Department of Biophysics, Dokuz Eylül University Medical School, 35340 Balcova-Izmir, Turkey*
[d] *Institute of Physiology, Medical University Lübeck, D-23538 Lübeck, Germany*
[e] *Brain Dynamics Research Network, TÜBITAK, Ankara, Turkey*

Accepted 1 May 2001

Abstract

This technical paper deals with the application of the Wavelet Transform to the study of evoked potentials. In particular, Wavelet Transform gives an optimal time-dependent frequency decomposition of the evoked responses, something difficult to be achieved with previous methods such as the Fourier Transform. We describe in detail the protocol for implementing the decomposition based on the Wavelet Transform and apply it to two different types of evoked potentials. In the first case we study alpha responses in pattern visual evoked potentials and in the second case, we study gamma responses to bimodal (auditory and visual) stimulation. Although in this study we focus on methodological issues, we briefly discuss physiological implications of the present time–frequency analysis. Furthermore, we show examples of the better performance of the wavelet decomposition in comparison with Fourier-based methods.

Theme: Sensory systems

Topic: Auditory systems: central physiology

Keywords: Wavelet; Fourier; EEG; Evoked potential; Brain oscillation; Alpha band; Gamma band; Entropy

1. Type of research

Evoked potentials (EPs), or more generally, event-related-potentials (ERPs) are defined as the changes the electroencephalogram (EEG) undergoes when a certain event occurs, e.g. when a sensory stimulus is applied. It has been proposed [3] that EPs appear as a reorganization of the spontaneous brain oscillations in response to the stimulus. Supporting this view, several works (see Refs. [4,7] and references therein) showed changes in different frequency bands upon stimulation. Moreover, these changes have been related with different sensory and cognitive processes.

Since the frequency content of EPs is time dependent, new methods of time–frequency analysis have been implemented. In the present study we show the advantages of the Wavelet Transform in comparison with Fourier-based filtering for the analysis of the time varying frequency composition of evoked potentials. For two different data sets we will study changes in the alpha band (8–16 Hz) in the first case, and in the gamma band (32–64 Hz) in the second case. Here we will just focus on methodological issues since physiological meanings of these results were already discussed elsewhere [16,21].

2. Time required

Time required for processing of the data increases linearly with the number of data points. We remark that the

*Corresponding author. Tel.: +49-2461-612302; fax: +49-2461-612430.

E-mail address: r.quianquiroga@fz-juelich.de (R. Quian Quiroga).

1385-299X/01/$ – see front matter
PII: S1385-299X(01)00077-0

processing time is even faster than the Fast Fourier Transform, which requires of the order of $N*\log(N)$ (N: number of data points).

3. Material and methods

The present article is focused on results obtained with the method applied to two different data sets. In the first data set (pattern visual EPs, 10 healthy subjects) we will analyze changes upon stimulation in the alpha band (8–16 Hz) and in the second data set (bimodal EPs, 15 healthy subjects) the ones of the gamma band (32–64 Hz). In both cases the sampling rate was 500 Hz and after band pass filtering in the range 0.1–70 Hz, about 2 s of data for each single trial (512 data pre- and 512 data post-stimulation) were saved on hard disk.

3.1. Pattern visual evoked potentials

In a first session (no-task visual evoked potentials, VEP) subjects were passively watching a checkerboard light pattern (sidelength of the checks 50′), the stimulus being a checker reversal ($n=100$ stimuli). In the second session, two different visual stimuli were presented in a pseudo-random order (oddball paradigm; $n=200$ stimuli): 75% of the stimuli were the so called 'non-target' (NT, a color reversal of the checks) and the other 25% were the deviant stimuli or 'target' (T, also a color reversal but with a half check displacement of the pattern). Subjects were instructed to ignore the non-target stimuli and to count the number of appearances of the target ones (see Ref. [16] for more details on the experimental setup). Scalp recordings were obtained from frontal (F1, F2), central (C3, Cz, C4), parietal (P3, P4) and occipital (O1, O2) electrodes with linked earlobes reference. Inter-stimulus intervals varied randomly between 2.5 and 3.5 s.

3.2. Bimodal evoked potentials

Scalp recordings were obtained from frontal (F1, F2), central (C3, Cz, C4), temporal (T1, T2), parietal (P3, P4) and occipital (O1, O2) electrodes with linked earlobes references. Each subject was instructed to view and listen passively to the presented stimuli. A recording session was divided in three parts (see Ref. [21] for details): (a) the stimulus was a 2 kHz tone presented binaurally; (b) the stimulus was a rectangular light-step centered in the visual field; (c) the two previous stimulus were applied simultaneously (bimodal stimulation). In each case 120 stimuli were presented with pseudo-randomized inter-stimulus intervals ranging from 1 to 3 s.

3.3. Wavelet Transform: brief theoretical background

The Wavelet Transform (WT [12]) gives a time–frequency representation of a signal that has two main advantages over previous methods: (a) optimal resolution even in the time and frequency domains; (b) lack of the requirement of stationarity of the signal. It is defined as the convolution between the signal *x(t)* and the wavelet functions $\psi_{a,b}(t)$

$$W_{\psi}X(a,b) = \left\langle x(t) \,\middle|\, \psi_{a,b}(t) \right\rangle \tag{1}$$

where $\psi_{a,b}(t)$ are dilated (contracted) and shifted versions of a unique *wavelet function* $\psi(t)$

$$\psi_{a,b}(t) = |a|^{-1/2}\psi\left(\frac{t-b}{a}\right) \tag{2}$$

(*a, b* are the scale and translation parameters, respectively). The WT gives a decomposition of *x(t)* in different scales, tending to be maximum at those scales and time locations where the wavelet best resembles *x(t)*. Moreover, Eq. (1) can be inverted, thus giving the reconstruction of *x(t)*.

The WT maps a signal of one independent variable *t* onto a function of two independent variables *a, b*. This procedure is redundant and not efficient for algorithm implementations. In consequence, it is more practical to define the Wavelet Transform only at discrete scales *a* and discrete times *b* by choosing the set of parameters $\{a_j = 2^{-j};\ b_{jk} = 2^{-j}k\}$, with integers *j, k*.

Contracted versions of the wavelet function will match the high frequency components of the original signal and on the other hand, the dilated versions will match low frequency oscillations. Then, by correlating the original signal with wavelet functions of different sizes we can obtain the details of the signal at different scales. These correlations with the different wavelet functions can be arranged in a hierarchical scheme called multiresolution decomposition [14]. The multiresolution decomposition separates the signal into 'details' at different scales, the remaining part being a coarser representation of the signal called 'approximation'. Moreover, it was shown [14] that each detail (D_j) and approximation signal (A_j) can be obtained from the previous approximation A_{j-1} via a convolution with high-pass and low-pass filters, respectively.

4. Detailed procedure

A free software implementation in Matlab for doing the decomposition of the signal in frequency bands can be obtained from http://www.physio.mu-luebeck.de/user/rq/rq.htm. The procedure is as follows:

4.1. Artifact rejection

Trials contaminated with artifacts like blinking, head movements, muscle activity, etc. are identified by visual

Table 1
Filter coefficients corresponding to quadratic B-Spline wavelets

k	G (k)	H (k)	G′ (k)	H′ (k)
−10	0.0016	−0.0039		
−9	0.0191	−0.0342		
−8	−0.0050	0.0342		
−7	−0.0444	0.0793		
−6	0.0117	−0.0210		
−5	0.1033	−0.1840		
−4	−0.0259	0.0498	−0.0021	
−3	−0.2437	0.4239	0.0604	
−2	0.0340	−0.1403	−0.3063	0.25
−1	0.6552	−0.9004	0.6312	0.75
0	0.6552	0.9004	−0.6312	0.75
1	0.0340	0.1403	0.3063	0.25
2	−0.2437	−0.4239	0.0604	
3	−0.0259	−0.0498	0.0021	
4	0.1033	0.1841		
5	0.0117	0.0210		
6	−0.0444	−0.0793		
7	−0.0050	−0.0090		
8	0.0191	0.0342		
9	0.0016	0.0039		

G and H are the high-pass and low-pass filters, respectively. H′ and G′ are the inverse filters used for the reconstruction (from Ref. [1]).

inspection of the recording and eliminated for further analysis.

4.2. Choosing of the wavelet function

A basic wavelet function to be compared with the signal should be chosen. There are many different functions suitable as wavelets, each one having different characteristics that are more or less appropriate depending on the application. Indeed, the possibility of choosing the wavelet function to be compared with the signal is one of the main advantages of wavelets over Fourier-based methods. Irrespective of the mathematical properties of the wavelet to choose, a basic requirement is that it looks similar to the patterns to be localized in the signal. This allows a good localization of the structures of interest in the wavelet domain and moreover, it minimizes spurious effects in the reconstruction of the signal via the inverse Wavelet Transform. For this study, we choose quadratic B-Splines as mother functions due to their similarity with the evoked responses. We remark the following properties that make them optimal in signal analysis (see Refs. [9,24] for details): they are (anti-) symmetric, smooth, they have a nearly optimal time–frequency resolution and they have compact support. The filter coefficients associated with quadratic B-Splines are shown in Table 1. The first column corresponds to the high-pass filter G used to obtain the details and second column the ones of the low-pass filter H used to obtain the successive approximations. The third and fourth columns are the inverse filter coefficients used for reconstructing the signal.

4.3. Multiresolution decomposition of the signal

The procedure is schematically shown on the left side of Fig. 1.

(i) The convolution between the signal (the starting segment) and the filters G and H is calculated. Then, the signal is shifted one data point to the left and the previous calculation is repeated. This is done until the whole signal is covered. From this shifting we obtain a set of coefficients that represent how the wavelet function matches the signal in time.

(ii) Both sets of coefficients obtained by the convolution of the signal with the filters G and H are decimated by 2 (one every two data points is deleted). From this we obtain the first level detail D_1 (i.e. the high-pass filtered signal) and approximation A_1 (the low-pass filtered signal), respectively. Note that after decimation the number of data points of D_1 plus the ones of A_1 is equal to the number of data points of x, thus avoiding redundancy.

(iii) The first approximation is further decomposed; i.e. the two previous steps are repeated using the approximation as input signal. Note that decimation is analog to a

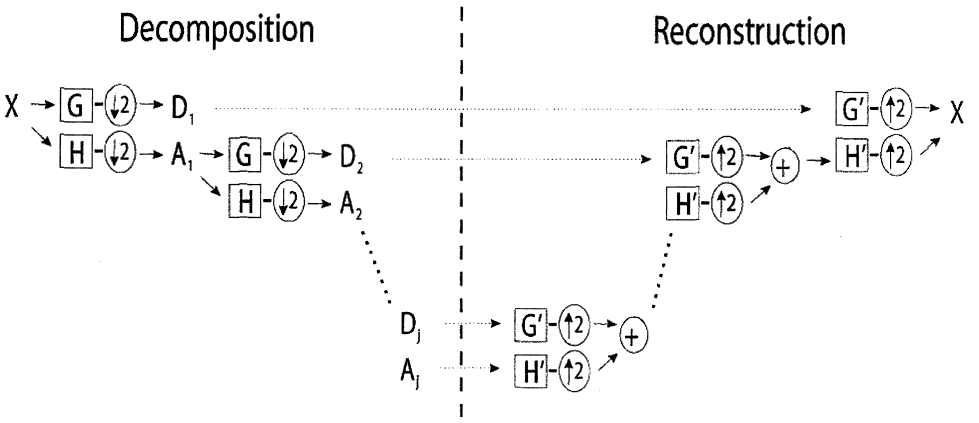

Fig. 1. Recursive implementation of the multiresolution decomposition and reconstruction. H and G are the low and high-pass filters, respectively, and H′ and G′ the inverse filters used for the reconstruction. Downward arrows mean decimation by 2 and upward arrows upsampling.

stretching of the mother function and therefore gives the comparison between the original signal and the wavelet function at different scales.

(iv) The previous three steps are repeated $j-1$ times, where j is the number of chosen levels. Then, the signal is decomposed into D_1 to D_j details and one final approximation A_j. In this study we used a 5-scale decomposition, thus obtaining coefficients in the following frequency bands: 62–125 Hz, 31–62 Hz (gamma), 16–31 Hz (beta), 8–16 Hz (alpha), 4–8 Hz (theta) and the last approximation giving the activity in the 0.5–4 Hz band (delta).

4.4. Reconstruction of the filtered signal

Reconstruction is done with convolution of the detail signals and the last approximation with the inverse filters G′ and H′. The procedure is schematically shown on the right side of Fig. 1. Since the goal is to obtain a filtered signal, reconstruction is done only from one scale.

(i) We choose the detail level from which we will do the reconstruction. For the alpha band this was the detail level 4, and for the gamma band the level 2. Then, the convolution between the chosen detail coefficients (the starting segment) and the filter G′ is calculated. If the reconstruction is to be done from the last approximation, instead of G′, H′ should be used. As before, the signal is shifted one data point to the left and the previous calculation is repeated until reaching the last coefficient.

(ii) The data obtained from the previous step is upsampled by inserting zeros between samples (this is the inverse to decimation).

(iii) The previous two steps are repeated $j-1$ times (j is the scale from which the reconstruction is done) but now using the filter coefficients H′. This gives the reconstructed signal filtered in the frequency band corresponding to the scale j.

As an example, Fig. 2 shows the multiresolution decomposition obtained from an averaged pattern visual EP (electrode O1) of a typical subject upon TARGET stimulus. The left part of the figure shows the wavelet coefficients and the right part shows the corresponding reconstructed waveforms. In the first 300 ms we observe an increase in the alpha and theta bands (D_4, D_5) correlated with the first waves appearing in the average EP (P100–N200). Only upon target stimulus, there is an increase in the delta band (A_5) correlated with the positive wave at 300 ms (P300).

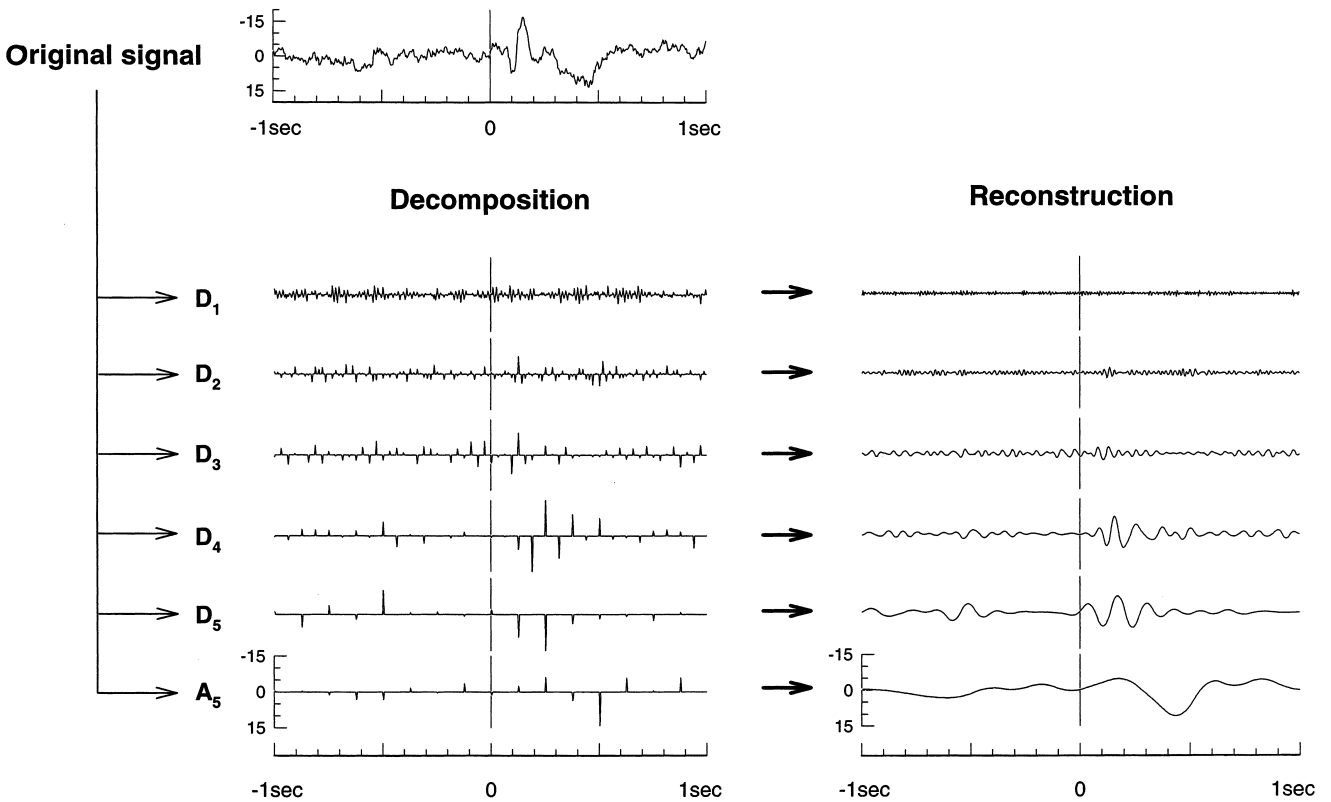

Fig. 2. Five-level multiresolution decomposition of an average evoked potential from a typical subject (electrode O2, target stimulus). D_1 to D_5 are the detail signals and A_5 is the last approximation. The wavelet coefficients show how closely the signal matches locally the different dilated versions of the wavelet 'mother function' (in this case a quadratic B-Spline). Furthermore, by applying the inverse transform, the signal can be reconstructed from the wavelet coefficients for each scale. Along the y-axis, values are in μV for the original signal and the reconstructed signals, and in arbitrary units for the wavelet coefficients.

5. Results

5.1. Advantages over digital filtering

Fig. 3 gives some examples of single-trial evoked potentials, in which results obtained with the Wavelet Transform and with digital filtering are compared. We would like to remark that the sweeps selected do not necessarily show a clear evoked response, but they are suitable for showing the better resolution achieved with the multiresolution decomposition based on the Wavelet Transform in comparison with conventional digital filtering. The digital filter used was an 'ideal filter' (i.e. bandpass filtering in the Fourier domain, as used in several earlier papers [3]) with the filter limits set in agreement with those obtained with the multiresolution decomposition for the alpha band.

As a general remark we can state that with wavelets a better resolution and localization of the features of the signal is achieved. In sweep #1, in between the dotted vertical lines, a transient with a frequency clearly lower than the range of alpha band is shown. The digital filtering does not resolve this transient and it spuriously 'interpolates' alpha oscillations in continuity with the ones that precede or follow the transient. On the other hand, the Wavelet coefficients and the reconstructed waveform from these coefficients show a decrease in this time segment. Something similar occurs in sweep #2 with the transient marked with an arrow. In fact, this transient is due to the cognitive P300 wave typically obtained upon target stimuli. As in the original signal, we observe with wavelets that there is no important contribution of alpha oscillations in this time range. On the contrary, the digital filter has not enough resolution for resolving this. The better time–frequency resolution of wavelets (in this case a better frequency localization for a certain time range) can be also seen in sweep #3. In the original signal, in between the vertical dotted lines there is a marked oscillation of about 4–6 Hz corresponding to the theta band. The digital filtered signal shows an alpha oscillation not present in the

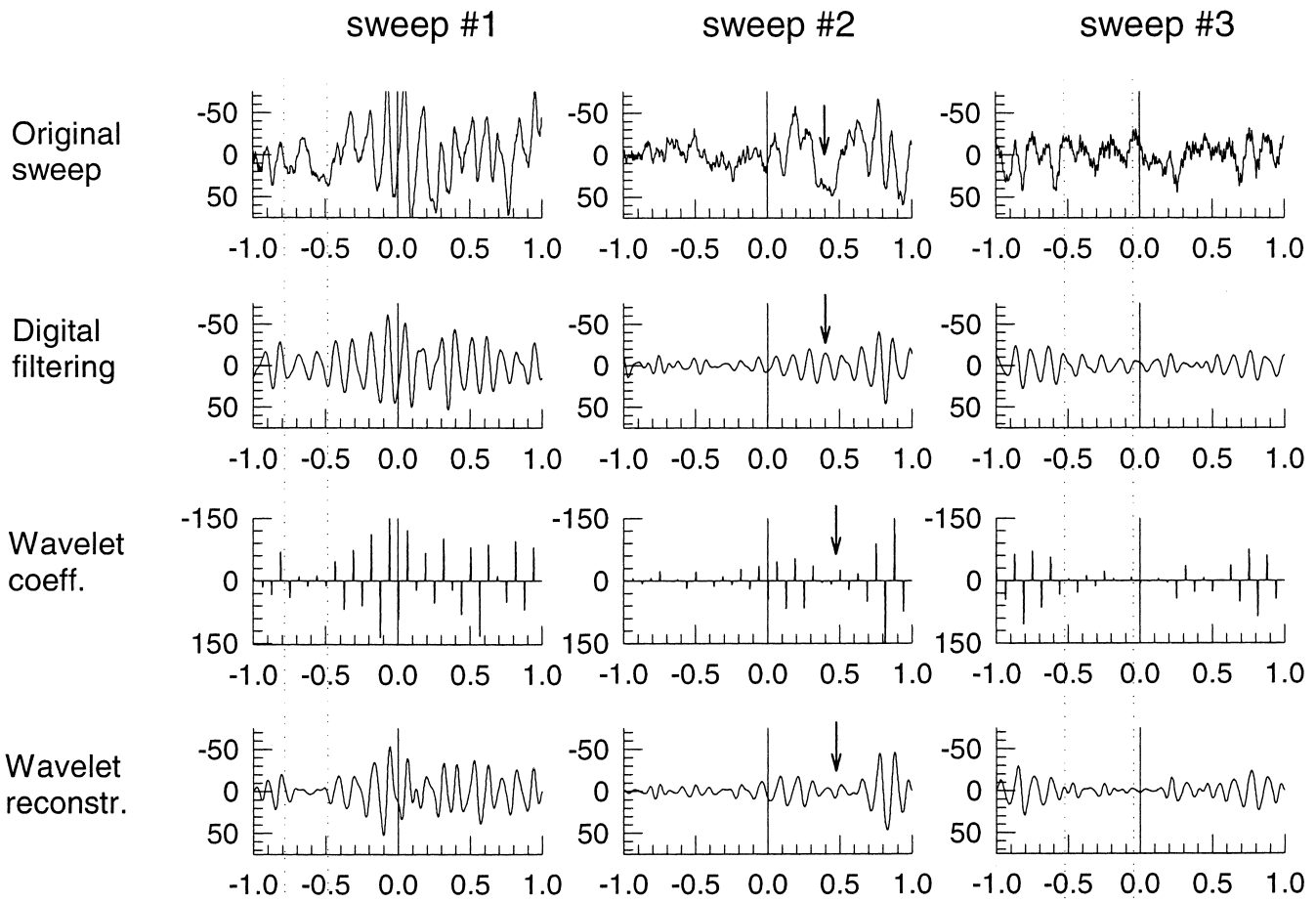

Fig. 3. Three examples (single sweeps) of the better performance obtained with the Wavelet Transform in comparison with conventional digital filtering. The first row shows the original signal, the second row the result after a digital filtering in the alpha range (8–16 Hz) and the last two rows show the wavelet coefficients in the alpha band and the reconstruction of the signal from the coefficients.

original signal. Again, due to its better resolution the wavelet coefficients and the reconstructed signal show a clear decrease in alpha for this time range.

5.2. Alpha responses in pattern visual evoked potentials

The grand average (across subjects) evoked responses are shown in left side of Fig. 4. Upper plots correspond to the responses to no-task stimulation (VEP), middle plots to non-target (NT) stimuli and lower plots to target (T) stimuli. Only left electrodes and Cz are shown, the responses of the right electrodes being qualitatively similar. A positive deflection at about 100 ms after stimulation, followed by a negative rebound (the P100–N200 complex) is clearly visible in all modalities, best defined in occipital locations. Target stimulation led to a marked positive peak between 400 and 500 ms (P300), related with the processes involved in the performance of the task (i.e. counting the number of target appearances).

Middle and right plots of Fig. 4 show the alpha band wavelet coefficients and the filtered EPs reconstructed from these coefficients respectively. Amplitude increases after stimulation were distributed over the entire scalp for the three stimulation types, having a better definition in the occipital electrodes. Furthermore, in posterior electrodes responses upon target stimulation are prolonged compared with the other two modalities. A multiple factor analysis of variances (MANOVA) showed no significant differences between stimulus type. Electrode differences, instead, were significant, confirming the predominant localization of the enhancements in the occipital locations, with a lower amplitude response in the anterior electrodes ($P<0.01$).

The delay of the maximum response in occipital electrodes was of about 180 ms after stimulation. In parietal electrodes the maximum appeared about 30 ms later, and in central and frontal electrodes between 50 and 100 ms after the occipital one. MANOVA test showed significant delays for frontal and central responses in comparison to the occipital ones ($P<0.05$).

5.3. Gamma responses in bimodal evoked potentials

Evoked gamma-range (31–62 Hz) EEG-oscillations are related with the processes originating from audio-visual stimulation, i.e. gamma-range time–frequency responses are contained in unisensory (auditory, visual; AEP, VEP) and bisensory (audio-visual; BEP) evoked potentials.

The grand average of $n=15$ subjects is shown in Fig. 5. Wavelet coefficients according to each stimulus condition (AEP, VEP, BEP) and electrode position are displayed for their pre-stimulus (-0.5 s) and post-stimulus (0.5 s) course. For sake of simplicity only right-hemispheric recordings (F4, C4, P4, O2) and Cz are shown. With auditory stimulation, enhancements are visible in central locations and more poorly defined in the occipital ones. Visual stimulation shows enhancements only in C4 and Cz. On the other hand, bimodal stimulation evokes significantly higher enhancements than the other two modalities. These enhancements occur about 64 ms after stimulus and last up to 160 ms. They are distributed diffusely in the surface EEG. However, bimodal responses are most overt in central electrodes and especially in the frontal ones, where enhancements occur upon bimodal stimulation exclusively. Regardless of location, *increases* in BEP gamma-range components are significantly higher when compared to AEP and VEP (paired *t*-tests, $P<0.01$, respectively). Furthermore the increases in BEP are significantly greater than the linear sum of AEP and VEP (AEP + VEP).

6. Discussion

Briefly, alpha responses to pattern visual EPs were distributed through the whole scalp, best localized in occipital locations. Alpha responses gained great attention in the last decade (see Refs. [5,8]). The fact that alpha amplitude increases were independent of the type of stimulus (therefore not changing upon cognitive processes related with target stimulus) as well as their maximal and earliest appearance in occipital locations (the primary visual sensory area) points at a functional relevance in sensory processing (for a more detailed discussion see Refs. [8,16]).

Gamma amplitude increases upon bimodal stimulation were larger and appeared earlier than the ones obtained with both unimodal stimuli. Furthermore, bimodal responses were not a superposition of the auditory and visual ones. Then, a new behavior solely related with the appearance of both stimuli together should be considered. We hypothesize (see Ref. [21] for more details) that this fast activity is responsible of transmitting the information that two different stimuli are manifestations of the same process. Rather than stressing physiological meanings of these results we would like to remark that physiological interpretations highly rely on the optimal time–frequency allowed by the Wavelet Transform.

6.1. Trouble-shooting

When making the convolution of the original signal with the wavelet function, one should define how to deal with the borders (i.e. at the beginning and at the end of the signal there are not enough data points to be compared with the wavelet function). In our case, we extended each single trial with data from the neighboring trials. This introduces some distortion in the borders. For this reason each single trial should have enough data points preceding and following the evoked responses in order to have this distortion outside the zone of interest. For the type of

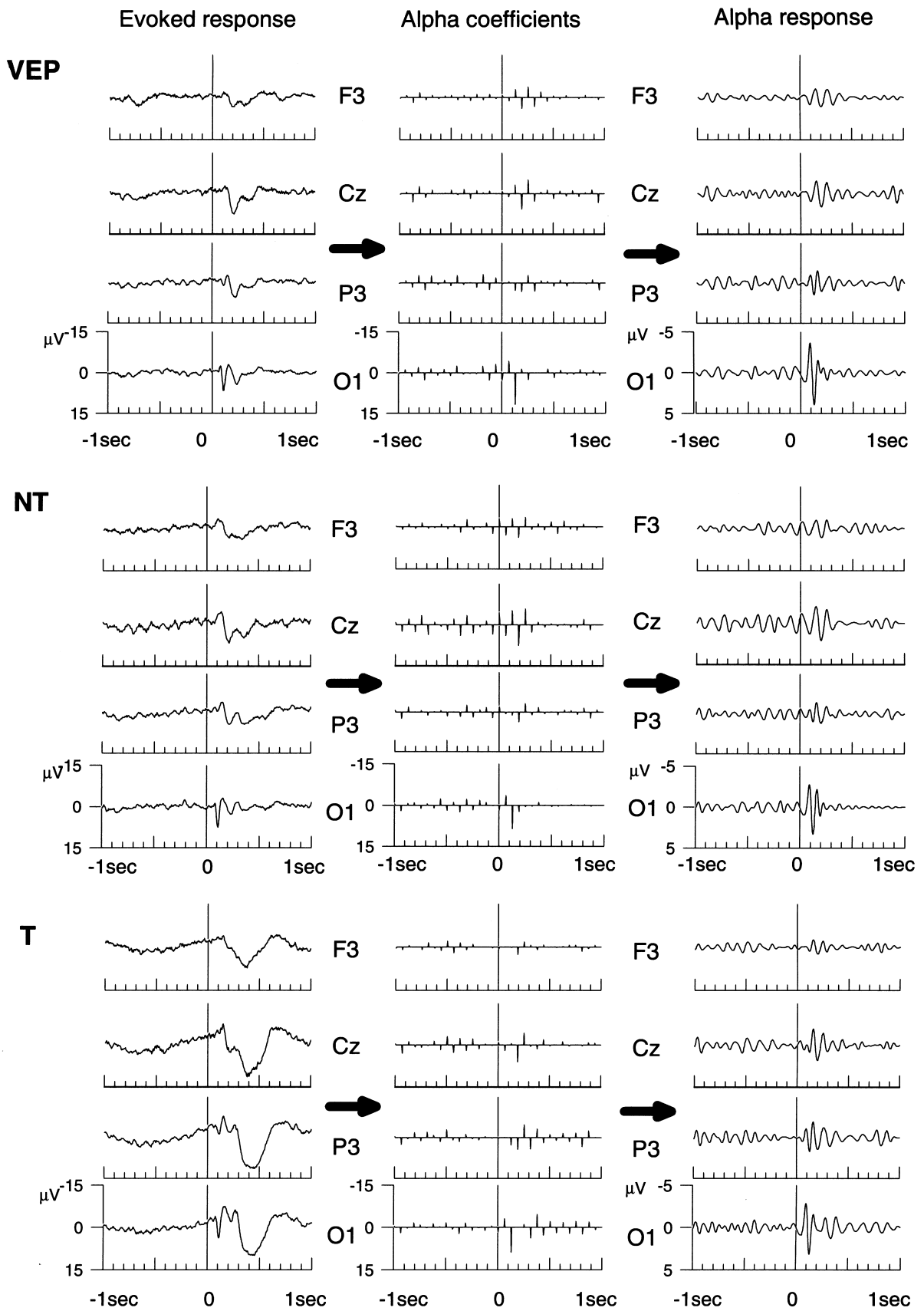

Fig. 4. Evoked responses (left side), wavelet coefficients of the alpha band (middle) and filtered evoked potentials reconstructed from these coefficients (right side). Upper plots correspond to no-task stimulation (VEP), middle plots to non-target stimulus (NT) and lower plots to the target ones (T). Only left electrodes and Cz are shown, the right electrodes having a similar response pattern.

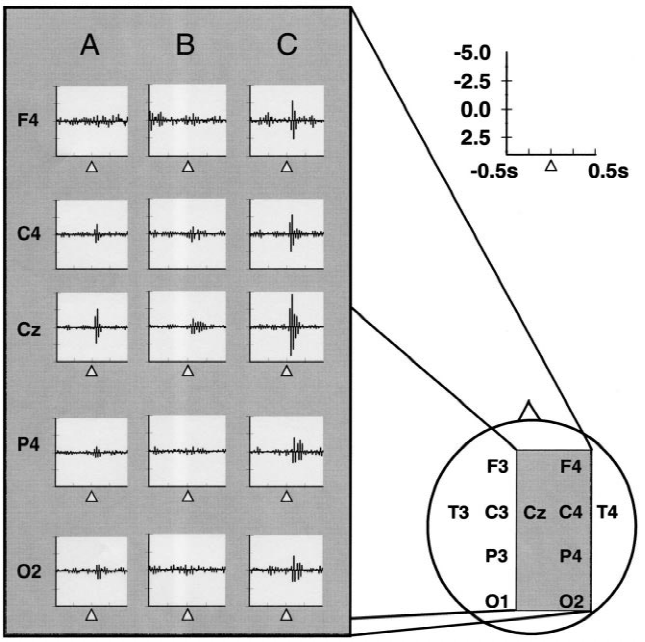

Fig. 5. Grand average of the gamma band (31–62 Hz) wavelet coefficients in $n=15$ subjects. Only right-hemispheric recordings (F4, C4, P4 and O2) and Cz shown. Along the x-axis 0.5 s pre- and post-stimuli are plotted with y-values in arbitrary units. A, auditory evoked potentials; B, visual evoked potentials; C, bisensory evoked potentials.

evoked potentials analyzed in this study it is suggested to have at least 0.5 s before and 1 s after stimulation stored.

6.2. Alternative and support protocols

The first method of choice for analyzing EP responses in different frequency bands is a 'Fourier-based' digital filtering. However, as shown in Section 5, non-optimal time–frequency resolution of conventional filters can produce spurious results that can be avoided by using the Wavelet Transform. We would like to remark two advantages of the Wavelet Transform in comparison with Fourier-based methods. First, Wavelet Transform lacks the requirement of stationarity, this being crucial for avoiding spurious results when analyzing brain signals, already known to be highly nonstationary. Second, a better time–frequency resolution can be achieved. This is very important in the case of EPs, where the relevant responses usually take place in a relative short time. However, we would like to mention that a first analysis of the data with Fourier-based methods, such as with the method of Transient Response and Amplitude Frequency Characteristics [3], is advantageous in order to visualize all frequency responses together. This is an important help to first analyze the global behavior of the responses in the frequency domain, prior to their analysis in frequency bands with the Wavelet Transform.

Several protocols similar to the one described in our study use different sets of wavelet coefficients for analysis purposes. Among others, this approach had already been used for automatically detecting spike complexes [22], for doing selective averages of the P300 responses [10], for distinguishing between normal and demented subjects [1], for classifying different type of single trials responses [6] and for measuring phase locking between single trials [17]. As presented in this study, the wavelet decomposition has been used for defining functional properties of EP frequency components [6,13,16,21,23]. Moreover, from the distribution of the wavelet coefficients in the different frequency bands, a time-varying definition of entropy has been proposed [15]. This entropy measure allowed the study of the ordering, in the frequency domain, of the ongoing background EEG activity upon stimulation [15,19,20]. Finally, sets of wavelet coefficients have been correlated with different EPs and they have being used for filtering the ongoing EEG activity, leading to the identification of the EPs at the single-trial level [2,11,18].

7. Quick procedure

1. Rejection of trials with artifacts
2. Choosing of the wavelet function to be used
3. Multiresolution decomposition of the EPs
4. Filtered reconstruction of the EPs from the chosen scale (corresponding to a frequency band)

Acknowledgements

We are thankful to Prof. Peter Grasberger for corrections on this manuscript. Part of the results presented were calculated with software developed by Prof. Tamer Demiralp and Dr. Ahmed Ademoglu, to whom we are indebted.

References

[1] A. Ademoglu, E. Micheli-Tzanakou, Y. Istefanopulos, Analysis of pattern reversal visual evoked potentials by spline wavelets, IEEE Trans. Biomed. Eng. 44 (1997) 881–890.
[2] E.A. Bartnik, K.J. Blinowska, P.J. Durka, Single evoked potential reconstruction by means of wavelet transform, Biol. Cybern. 67 (1992) 175–181.
[3] E. Basar, EEG-Brain Dynamics. Relation Between EEG and Brain Evoked Potentials, Elsevier, Amsterdam, 1980.
[4] E. Basar, T. Bullock (Eds.), Induced Rhythms in the Brain, Birkhauser, Boston, 1992.
[5] E. Basar, R. Hari, F.H. Lopes da Silva, M. Schürmann, Brain alpha activity – new aspects and functional correlates, Int. J. Psychophysiol. 26 (1997) 1–482.
[6] E. Basar, T. Demiralp, M. Schürmann, C. Basar-Eroglu, A. Ademoglu, Oscillatory brain dynamics, wavelet analysis and cognition, Brain Lang. 66 (1999) 146–183.
[7] E. Basar, Brain Oscillations, Principles and Approaches; Integrative Brain Function: Neurophysiology and Cognitive Processes, Brain Function and Oscillations, Vols. I and II, Springer, Berlin/Heidelberg/New York, 1999.

[8] E. Basar, C. Basar-Eroglu, S. Karakas, M. Schürmann, Event-related oscillations in perception and memory, Int. J. Psychophysiol. 39 (2001) 87–256.
[9] C. Chui, An Introduction To Wavelets, Academic Press, San Diego, CA, 1992.
[10] T. Demiralp, A. Ademoglu, M. Schürmann, C. Basar-Eroglu, E. Basar, Detection of P300 waves in single trials by the wavelet transform, Brain Lang. 66 (1999) 108–128.
[11] A. Effern, K. Lehnertz, T. Schreiber, P. David, C.E. Elger, Nonlinear denoising of transient signals with application to event related potentials, Physica D 140 (2000) 257–266.
[12] A. Grossmann, J. Morlet, Decomposition of Hardy Functions into square integrable wavelets of constant shape, SIAM J. Math. Anal. 15 (1984) 723–736.
[13] V. Kolev, T. Demiralp, J. Yordanova, A. Ademoglu, U. Isoglu-Alkac, Time–frequency analysis reveals multiple functional components during oddball P300, Neuroreport 8 (1997) 2061–2065.
[14] S. Mallat, A theory for multiresolution signal decomposition: the wavelet representation, IEEE Trans. Pattern Anal. Machine Intell. 2 (1989) 674–693.
[15] R. Quian Quiroga, O.A. Rosso, E. Basar, Wavelet-entropy: a measure of order in evoked potentials, Electr. Clin. Neurophysiol. 49 (Suppl.) (1998) 298–302.
[16] R. Quian Quiroga, M. Schürmann, Functions and sources of event-related EEG alpha oscillations studied with the Wavelet Transform, Electroencephalogr. Clin. Neurophysiol. 110 (1999) 643–655.
[17] R. Quian Quiroga, E. Basar, M. Schürmann, Phase locking of event-related alpha oscillations, in: K. Lehnertz, C.E. Elger, J. Arnhold, P. Grassberger (Eds.), Chaos in Brain? World Scientific, 2000.
[18] R. Quian Quiroga, Obtaining single stimulus evoked potentials with wavelet denoising, Physica D 145 (2000) 278–292.
[19] R. Quian Quiroga, O.A. Rosso, E. Basar, M. Schürmann, Wavelet entropy in event-related potentials: a new method shows ordering of EEG oscillations, Biol. Cybern. (2001), in press.
[20] O.A. Rosso, S. Blanco, J. Yordanova, V. Kolev, M. Schürmann, E. Basar, Wavelet entropy: a new tool for analysis of short time brain electrical signals, J. Neurosci. Methods 105 (1) (2001) 65–75.
[21] O. Sakowitz, R. Quian Quiroga, E. Basar, M. Schürmann, Bisensory stimulation increases gamma-responses over multiple cortical regions, Cogn. Brain Res. (2001), in press.
[22] S. Schiff, A. Aldroubi, M. Unser, S. Sato, Fast wavelet transformation of EEG, Electroencephalogr. Clin. Neurophysiol. 91 (1994) 442–455.
[23] A. Tzelepi, T. Bezerianos, I. Bodis-Wollner, Functional properties of sub-bands of oscillatory brain waves to pattern visual stimulation in man, Clin. Neurophysiol. 111 (2000) 259–269.
[24] M. Unser, A. Aldroubi, M. Eden, On the asymptotic convergence of B-Spline wavelets to Gabor functions, IEEE Trans. Inf. Theory 38 (1992) 864–872.